# Velocity analysis from interferometric data

*Eric A. Dussaud* and William W. Symes*

## Summary

Velocity analysis resolves relatively long scales of earth structure, typically wavelengths larger than 500m. Migration produces images with length scales on the order of 10's of m. In between these two scale regimes lies another, in which the resolution of velocity analysis is uncertain and the energy of images is small to non-existent. We propose a version of differential semblance based on cross-correlations of seismic traces that is essentially insensitive to the noise in seismic reflection data associated with the middle scale in velocity heterogeneity.

## Introduction

Seismic imaging techniques typically resolve the long-scale component of velocity (wavelengths larger than 500m) via the process of velocity analysis, whereas migration (i.e. linearized inversion) methods resolve the high-frequency component of the velocity (the reflectivity, typically on the order of 10's of m). However, standard techniques do not estimate the intermediate scale in velocity heterogeneity. In fact, seismic data simply do not contain any reliable information on this intermediate scale structure (Jannane et al., 1989; Claerbout, 1985). Although the scale gap indicates that seismic data are less sensitive to the middle scales of velocity than they are to the long or wavelength scales, the nonlinearity of the seismic problem suggests than the associated "energy" or (lack of) "information" would cascade between scales and pollute the estimation of the long-scale component (velocity analysis) and the quality of the other (migration). Because these middle scales of velocity are neither imaged by migration nor extracted from velocity analysis, they must be regarded as random perturbations. In this paper, we are interested in assessing the effects these random perturbations have on the estimation of the long-scale component of velocity.

Borcea et al. (2002; 2003; 2004) have proposed various *statistically stable* functions of random wavefields (solutions of the wave equation when the coefficients are random spatial fields). Their definition of "statistically stable" is asymptotic: a function is statistically stable if random fluctuations of size (suitably measured) $\epsilon$ lead to fluctuations in the function values of size $\epsilon^p$ with $p > 1$, i.e. the variance of the function is asymptotically negligible compared to the random coefficients. It should be noted that the wavefield itself is never statistically stable. However, Borcea et al. (2002; 2003; 2004) have shown that *cross-correlations of neighboring time traces* are statistically stable under various circumstances. The importance of using cross-correlations of neighboring traces stems from the fact that doing so achieves the desired random phase cancellations which are ultimately responsible for the statistical stability.

In this paper, we show that cross-correlations of (reflection) seismic data do contain moveout information, and suggest a functional of the differential semblance type that can be optimized to reconstruct the background medium from them (Carazzone and Symes, 1991; Symes, 1993; Symes, 1998). Because the functional uses interferometric data, it is therefore stable in the sense explained above. Theoretical justification of this assertion required an extension of the results of Borcea et al. (2002; 2003; 2004), which will be reported elsewhere. The version described in this abstract is realized using convolutional layered modeling, as it simplifies both theory and numerics. However, extension to more complex models can be done, at the expense of more complex mathematical machinery.

The next section briefly presents the well-known convolutional model, which provides a simple framework within which to pose the velocity analysis problem (Symes, 1999). The following section contains the description of the differential semblance functional. We then proceed to show the success of the method, using a synthetic data example created from the Marmousi model. We end the paper with a brief indication of how the method may be generalized to more complex models.

## The convolutional model for layered media

For both theoretical and numerical results presented in this paper, we will use the asymptotic linearized model of scattering from a layered medium. The most convenient form of this model parametrizes velocity and reflectivity by vertical 2-way travel time $t_0$ rather than depth $z$ and uses the interval velocity $v(t_0)$ as the basic velocity representation. For a particular choice $v^*$ of $v$ and reflectivity $r^*$, the noise-free convolutional model is:

$$d^*(t,h) = r^*\left(T_0^*(t,h)\right) \tag{1}$$

Here $t$ represents the time, $h$ is the half-offset, and $d(t,h)$ is a common midpoint gather. The time-to-depth conversion function $T_0(t,h)$ is related to the 2-way traveltime function $T(t_0,h)$ by:

$$T_0\left(T(t_0,h),h\right) = t_0, \quad T(t_0,h) = \sqrt{t_0^2 + h^2 v_{\mathrm{RMS}}^{-2}(t_0)} \tag{2}$$

Here $v_{\mathrm{RMS}}$ is the RMS velocity profile corresponding to $v$. Note that we explicitly use the hyperbolic moveout approximation to the traveltime function. We also ignored filtering by the source wavelet, which gives the convolutional model its name, and the amplitude factors. The goal of velocity analysis is to determine moveout, which neither wavelet nor amplitude variation with offset strongly affect. For a complete derivation of the convolutional model from the wave equation, see Stolt and Weglein (1985).

## Differential semblance principle

The NMO operator, obtained from (1) by a simple inverse change of variables, corrects a CMP gather $d(t,h)$ for offset-dependent delay in the arrival times according to the formula:

$$r(t_0) \simeq d\left(T(t_0,h),h\right) \tag{3}$$

If the data are model-consistent (noise free) or differ from noise free data by slowly varying amplitudes, then:

$$\frac{\partial}{\partial h} d\left(T(t_0,h),h\right) \simeq 0$$

In other words, if $d(t,h) \simeq d^*(t,h)$, then the mean-square of the above expression, i.e.

$$\iint dh\, dt_0 \left| \frac{\partial T}{\partial h}(t_0,h) \frac{\partial d}{\partial t}\left(T(t_0,h),h\right) + \frac{\partial d}{\partial h}\left(T(t_0,h),h\right) \right|^2$$

should be approximately minimized when $v = v^*$. Changing variables from $t_0$ to $t$, i.e. setting $t_0 = T_0(t,h)$, we see that standard differential semblance optimization amounts to minimizing the functional:

$$\iint dh\, dt \left| p(t,h) \frac{\partial d}{\partial t}(t,h) + \frac{\partial d}{\partial h}(t,h) \right|^2$$

where we omitted the Jacobian factor, for simplicity. Here $p(t,h)$ denotes the ray parameter, i.e. the slowness of the ray passing offset $h$ at time $t$:

$$p(t,h) = \frac{\partial T}{\partial h}\left(T_0(t,h),h\right) \tag{4}$$

The formulation of standard differential semblance also includes a smoothing operator used to keep the spectrum of the differential semblance output comparable to that of the data (this operator annihilates the effect of differentiating the data, which enhances high-frequency content). To mimic this behavior, we will use time-integrated traces. Therefore the functional we propose to minimize has the form:

$$J[v] = \tfrac{1}{2} \iint dh\, dt \left| p(t,h) d(t,h) + b(t,h) \right|^2 \tag{5}$$

where we have set:

$$b(t,h) \equiv \int_{-\infty}^{t} \frac{\partial d}{\partial h}(\cdot,h), \tag{6}$$

In case the data are model-consistent, i.e. $d(t,h) \simeq d^*(t,h)$, then a short computation using (1), (2) and (6) shows that:

$$p(t,h)d(t,h) + b(t,h) \equiv \left[p(t,h) - p^*(t,h)\right] d(t,h)$$

Hence we obtain the equivalence:

$$J[v] \equiv \tfrac{1}{2} \iint dh\, dt \left|d(t,h)\right|^2 \left[p(t,h) - p^*(t,h)\right]^2 \tag{7}$$

That is, the functional $J[v]$ essentially measures the mismatch of event slowness weighted by data power. We can find another interpretation of the functional by expanding the integrand in (5) as follows:

$$I(h) = \int dt\, p^2(t,h) d^2(t,h) + 2p(t,h)d(t,h)b(t,h) + b^2(t,h)$$

Each term in the above expression may be viewed as a *weighted* cross-correlation. Indeed, defining

$$\begin{aligned}
I_1(t,h,h') &= \int ds\, p^2(s,h) d(t+s,h) d(s,h') \\
I_2(t,h,h') &= \int ds\, p(s,h) d(t+s,h) \left[\int_{-\infty}^{s} d(\cdot,h')\right] \\
I_3(t,h,h') &= \int ds \left[\int_{-\infty}^{s} d(t+\cdot,h)\right] \left[\int_{-\infty}^{s} d(\cdot,h')\right]
\end{aligned}$$

then clearly we have the following equivalence:

$$I(h) \equiv \left[ I_1 + 2\frac{\partial I_2}{\partial h'} + \frac{\partial^2 I_3}{\partial h \partial h'} \right]_{t=0,h'=h} \tag{8}$$

Hence the functional defined in (5) explicitly uses *infinitesimal* (weighted) cross-correlations of seismic traces. Because cross-correlations of nearby seismic traces with slowly-varying weights are stable against middle-scale fluctuations in the medium, the functional is stable against these fluctuations as well. The velocity analysis algorithm consists of determining the background model $v$ such that the functional $J[v]$ is minimized. Because the ray slowness $p$ is locally a smooth function of $v$, $J[v]$ is a smooth function of $v$ as well, and can therefore be optimized by local optimization techniques. A similar analysis would show that the gradient $\nabla J[v]$ is also stable against middle-scale fluctuations. Thus the velocity analysis algorithm is statistically stable, and should therefore yield kinematically accurate background velocities despite the fluctuations at the middle scale.

## Synthetic Data Trials

The trials reported in this section are based on 2-D synthetic data sets created using linearized acoustic simulations (Born modeling). We created a model with three distinct scales of velocities. First, we extracted a 1-D velocity profile from the well known Marmousi model (Bourgeois et al., 1991). The background velocity was chosen as the linear average of this profile. Subtraction of this linear background from a smoothed version of the original profile (obtained by convolution with a kernel of smoothing width equal to 100m) resulted in a reflectivity varying on a scale of about 100m. Both the background model and the reflectivity were then extended to 2-D layered models. The middle scale fluctuations were generated as realizations of a random process with a Gaussian correlation function (for its smoothness properties) having a characteristic correlation length of about 300m, thus creating Gaussian *blobs* of about 300m in size. The strength of the fluctuations was about 6% that of the background.

Figure 1 (top panel) shows the resulting CMP obtained when no fluctuations are added in the background. We used partially irregular grids (Dussaud and Symes, 2005) to describe the interval velocity as function of depth $z$. In this case, only two nodes were used as the background model is linear. The estimated reflectivity amounts to essentially NMO-corrected data in this setting. Figure 1 (middle panel) shows that this gather is almost perfectly flat. Figure 1 (bottom panel) displays the estimated RMS velocity overplotted on a standard velocity spectrum (produced using Seismic Unix' `suvelan` utility). The estimated RMS velocity passes directly through the velocity spectrum peaks corresponding to the reflectors.

Figure 2 (top panel) shows a typical CMP obtained for a particular realization of the random medium when middle scale fluctuations are added to the background model. The effect of the fluctuations can be measured by random phase shifts in the data. Figure 2 (middle panel) shows the inverted reflectivity. The estimated RMS velocity, shown in the bottom panel, appears to have changed little from the case illustrated on Figure 1, suggesting that the algorithm was not sensitive to the fluctuations in individual trace arrival times.

## Conclusions

This paper has demonstrated an (automatic) velocity analysis algorithm based on cross-correlations of seismic data which is essentially insensitive to the noise in seismic reflection data associated with the middle scale in velocity heterogeneity. This paper represents the preliminary report of an ongoing project. Testing is underway to quantitatively verify the statistical stability of differential semblance and the associated velocity estimates in the asymptotic, statistical sense specified by Borcea et al. (2002; 2003; 2004). Differential semblance has been applied with success to estimation of laterally heterogeneous velocity models, using for example Kirchhoff migration as the underlying imaging engine, rather than NMO (Chauris and Noble, 2001). Extension of the theory predicting statistical stability of trace cross-correlations in the laterally heterogeneous setting would then suggest that differential semblance 2D and 3D velocity macro-model estimates might inherit such stability.

## Acknowledgments

The authors would like to thank Liliana Borcea for many useful discussions and the sponsors of The Rice Inversion Project (TRIP) as well as ConocoPhillips for their support.

## References

Borcea, L., Papanicolaou, G. C., Tsogka, C., and Berryman, J., 2002, Imaging and time reversal in random media: Inverse Problems, **18**, no. 5, 1247–1279.

Borcea, L., Papanicolaou, G. C., and Tsogka, C., 2003, Theory and applications of time reversal and interferometric imaging: Inverse Problems, **19**, 139–164.

Bourgeois, A., Lailly, P., and Versteeg, R., 1991, The Marmousi model *in* Versteeg, R., and Grau, G., Eds., The Marmousi Experience:: IFP/Technip.

Carazzone, J., and Symes, W. W., 1991, Velocity inversion by differential semblance optimization: Geophysics, **56**, no. 5, 654–663.

Chauris, H., and Noble, M., 2001, Two-dimensional velocity macro model estimation from seismic reflection data by local differential semblance optimization: applications synthetic and real data sets: Geophys. J. Int., **144**, 14–26.

Claerbout, J. F., 1985, Imaging the earth's interior: Blackwell Scientific Publishers, Oxford.

Dussaud, E., and Symes, W. W., A sparse, bound-respecting parametrization of velocity models:, Technical Report 05-05, Department of Computational and Applied Mathematics, Rice University, Houston, Texas, USA, 2005.

Jannane, M., Beydoun, W., Crase, E., Cao, D., Koren, Z., Landa, E., Mendes, M., Picas, A., Noble, M., Roeth, G., Singh, S., Snieder, R., Tarantola, A., Trezeguet, D., and Xie, M., July 1989, Wavelengths of earth structures that can be resolved from seismic reflection data: Geophysics, **54**, no. 7, 906–910.

Papanicolaou, G., Ryzhik, L., and Solna, K., 2004, Statistical stability in time reversal: SIAM J. on Appl. Math., **64**, 1133–1155.

Stolt, R. H., and Weglein, A. B., 1985, Migration and inversion of seismic data: Geophysics, **50**, 2458–2472.

Symes, W. W., 1993, A differential semblance criterion for inversion of multioffset seismic reflection data: J. Geoph. Res., **98**, 2061–2073.

Symes, W. W., 1998, High frequency asymptotics, differential semblance, and velocity analysis: 68th Ann. Internat. Mtg., Expanded Abstracts, Soc. of Expl. Geophys.

Symes, W. W., All stationary points of differential semblance are asymptotic global minimizers: layered acoustics:, Technical Report 99-29, Department of Computational and Applied Mathematics, Rice University, Houston, Texas, USA, 1999.

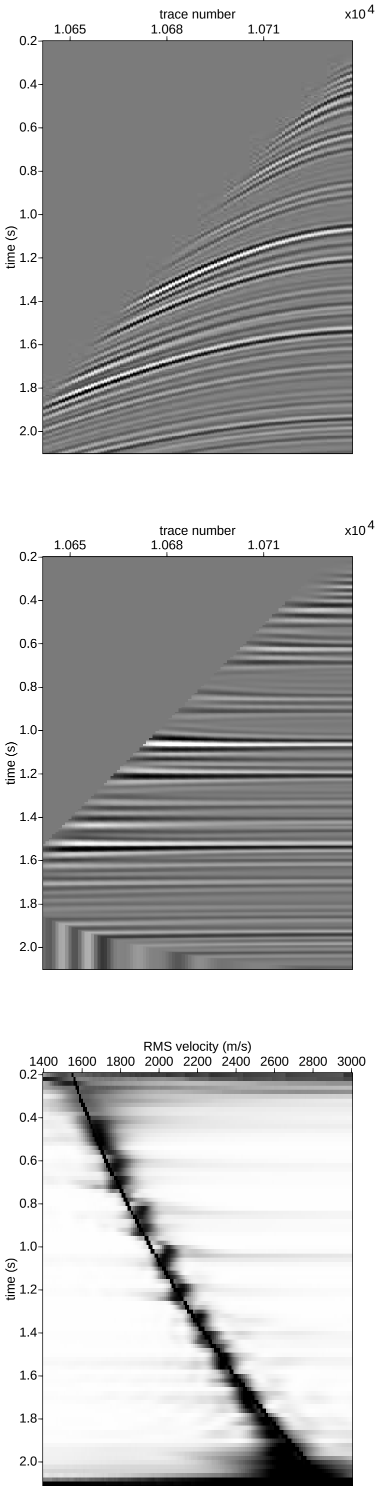


Fig. 1: Top: CMP. Middle: Inverted reflectivity at optimal DSO velocity. Bottom: Estimated RMS velocity (thick line) superimposed on velocity spectrum

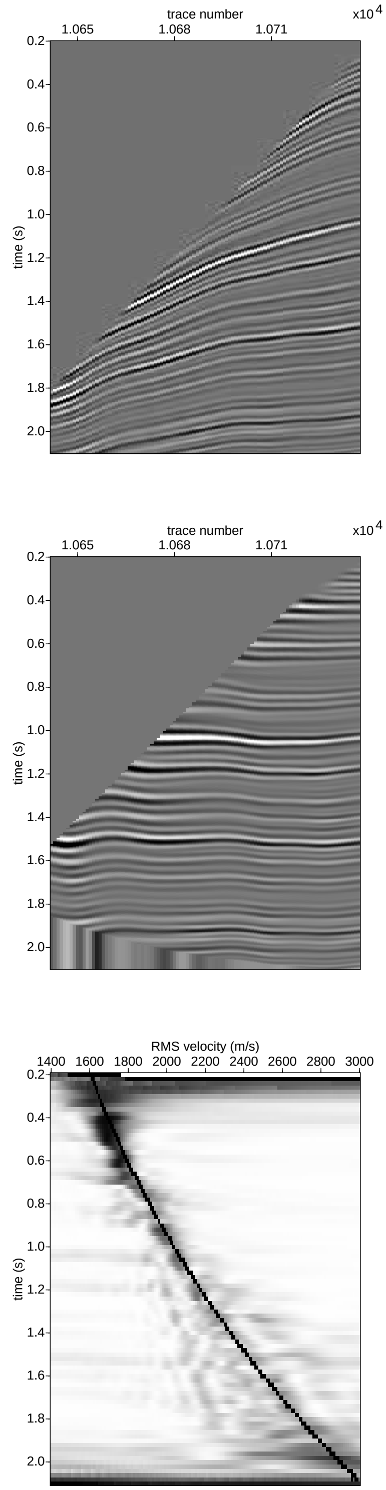


Fig. 2: Top: CMP . Middle: Common image gather at optimal velocity. Bottom: Estimated RMS velocity superimposed on velocity spectrum